

# SUM THROUGHPUT MAXIMIZATION FOR MULTI-TAG MISO BACKSCATTERING

Deepak Mishra and Erik G. Larsson

Div. Commun. Syst., Dept. of Electrical Engineering, Linköping University, 58183 Linköping, Sweden

## ABSTRACT

Backscatter communication (BSC) is emerging as the core technology for pervasive sustainable internet-of-things applications. However, owing to the resource-limitations of passive tags, this work targets at maximizing the achievable sum-backscattered-throughput by jointly optimizing the transceiver (TRX) design at the full-duplex multi-antenna reader and backscattering coefficients (BC) at the single antenna tags. Despite this joint optimization problem being non-convex, we present low-complexity joint TRX-BC designs by exploring the asymptotically-optimal solutions in low and high signal-to-noise-ratio regimes. We discourse that with precoder and detector designs at the reader respectively targeting downlink energy beamforming and uplink Wiener filtering operations, the BC optimization at tags can be reduced to a binary power control problem. Selected computer simulations are presented to validate the analytical claims, shed optimal-design insights, and demonstrate the throughput enhancement of around 20% over the relevant benchmark schemes.

**Index Terms**— Backscatter communication, precoder, MMSE, energy beamforming, power control, zero-forcing, antenna array

## 1. INTRODUCTION

Backscatter communication (BSC) technology, comprising of low-cost tags, without bulkier radio frequency (RF) chain components, can help in realizing the sustainable ultra-low-power networking [1]. Despite these potential merits, the widespread utility of BSC is limited by shorter read-range and lower achievable data rates [2]. These limitations can be overcome by using multiple antennas at the reader, which can help in separating out the backscattered signals from the multiple tags, and implement energy beamforming (EB) during carrier transmission. So, to fully utilize these gains, there is a need for investigating novel optimal transmit (TX) and receive (RX) beamforming at multi-antenna reader, and backscattering designs at tags.

### 1.1. State-of-the-Art

In BSC, the low-power tags communicate their information to the reader by respectively modulating their load impedances to control the strength, phase, or frequency of carrier signal(s) as received and reflected back to reader. Noting that the tags-to-reader uplink channel is coupled to the reader-to-tags downlink one, novel higher order modulation schemes were investigated in [3] for the monostatic multiple-input-single-output (MIMO) BSC settings. Whereas, considering a multi-antenna power beacon assisted bi-static BSC model, robust inference algorithms, not requiring any channel state information (CSI), were proposed in [4] to detect the sensing values of multiple single antenna backscatter sensors at a multi-antenna reader. Adopting the BSC model with multiple antennas at the reader, authors in [5] first presented maximum likelihood (ML) based optimal detector for simultaneously recovering the signals from emitter and tag. Then, they also considered suboptimal linear detectors (Maximum

Ratio Combining (MRC), Zero Forcing (ZF) and Minimum Mean-Squared Error (MMSE)), and the best-performing successive interference cancellation (SIC) based detectors. Investigating monostatic BSC between multi-antenna reader and single-antenna tag, least-squares and linear MMSE based channel estimates were derived in [6]. On different lines, with the goal of optimizing harvested energy among single-antenna tags, sub-optimal EB designs for multi-antenna reader were investigated in [7]. Thus, we realize that the research on utilizing the efficacy of multi-antenna reader based smart signal processing designs in multi-tag BSCs is still in its infancy.

Next we highlight a striking similarity between wireless powered communication networks (WPCN) [8–10] and BSC systems, which leads to a very similar throughput expression for the two systems, as can be noted from [10, eq. (4)] and (4) in Section 3, respectively. Actually, the energy transfer phase in WPCN to power-up the RF energy harvesting (EH) users has similar objective like the reader's carrier transmission to the tags for exciting them. Owing to this reason, the proposed TX-RX designs in this work for BSC can also be applied for sum-rate-maximization in WPCN with multi-antenna hybrid access point (HAP) and multiple single-antenna EH users [9, 10]. Further in Section 5, we show that our proposed design outperforms the ones designed for the multi-antenna HAP in [9, 10].

### 1.2. Motivation and Contributions

We observe that the requirements of RX design in uplink for efficient detection of the backscattered signals at the reader from multiple tags, are very different from those of the TX beamforming in downlink involving single-group multicasting-based carrier transmission. *To our best knowledge, the jointly-optimal transceiver (TRX) design for the multi-antenna reader has not been investigated yet. Also, the backscattering coefficient (BC) optimization at tags for maximizing the sum-backscattered-throughput (SBT) is missing.* Recently, a few BC design policies were investigated in [11] for maximizing the mean harvested power, due to the retro-directive EB at multi-antenna energy transmitter based on the backscattered signals from multiple single antenna tags. However, the possibility of efficient uplink backscattered information transfer from tags was ignored in [11].

In this work, we present novel analytical insights for optimal TRX and BC design, whose practical utility as targeted for monostatic multi-tag multiple-input-single-output (MISO) BSCs can also be easily extended for addressing the needs of WPCN and ambient or bi-static BSCs. These achievable longer read-range and higher SBT gains can thus enable widespread applicability of BSC technology in ultra-low-power emerging-radio networks like internet-of-things.

The three-fold contribution of this work is summarized below:

- Novel joint TRX designing at the reader and BC setting at the tags has been investigated for maximizing SBT from the multiple single-antenna tags in a monostatic MISO-BSC setting.
- Noting problem's non-convexity, we present low-complexity joint design based on the asymptotically-optimal solutions under the high and low signal-to-noise-ratio (SNR) regimes.

This work was supported in part by Swedish Research Council and ELLIIT.

- Numerical investigation is carried out to validate the analytical claims and quantify the achievable performance gains.

## 2. SYSTEM DESCRIPTION

We consider MISO monostatic BSC system comprising  $M$  single-antenna semi-passive tags  $\mathcal{T}_k, \forall k \in \mathcal{M} \triangleq \{1, 2, \dots, M\}$ , and one full-duplex reader  $\mathcal{R}$  equipped with  $N$  antennas. We assume that these  $M$  tags are randomly deployed in a square field of length  $L$  meters (m), with  $\mathcal{R}$  being at its center. To enable full-duplex operation [12], each of the  $N$  antennas at  $\mathcal{R}$  can transmit a carrier signal to the tags, while concurrently receiving the backscattered signals from them. In contrast to the practical challenges in implementing the full-duplex operation in conventional communication systems involving modulated information signals, the unmodulated carrier leakage in monostatic full-duplex BSC systems can be efficiently suppressed [12]. So  $\mathcal{R}$ , adopting linear precoding, assigns each  $\mathcal{T}_k$  a precoder  $\mathbf{f}_k \in \mathbb{C}^{N \times 1}$  and simultaneously transmits  $M$  independent and identically distributed (IID) symbols,  $\mathbf{s}_{\mathcal{R}} \sim \mathcal{CN}(\mathbf{0}_{M \times 1}, \mathbf{I}_M)$ . The resulting  $M$  modulated reflected data symbols, as simultaneously backscattered from  $M$  tags, are then respectively spatially separated by  $\mathcal{R}$  with the aid of  $M$  linear decoding vectors as denoted by  $\mathbf{g}_k \in \mathbb{C}^{N \times 1}, \forall k \in \mathcal{M}$ , where  $\mathbf{g}_k$  is used for decoding  $\mathcal{T}_k$ 's message.

The  $\mathcal{T}_k$ -to- $\mathcal{R}$  wireless reciprocal-channel is denoted by an  $N \times 1$  vector  $\mathbf{h}_k \sim \mathcal{CN}(\mathbf{0}_{N \times 1}, \beta_k \mathbf{I}_N), \forall k \in \mathcal{M}$ . Here, parameter  $\beta_k$  represents average channel power gain incorporating the fading gain and propagation loss over  $\mathcal{T}_k$ -to- $\mathcal{R}$  or  $\mathcal{R}$ -to- $\mathcal{T}_k$  link. For implementing the backscattering operation, we consider that each  $\mathcal{T}_k$  modulates the carrier received from  $\mathcal{R}$  via a complex baseband signal denoted by  $x_{\mathcal{T}_k}$  [13], which includes a structure-dependent constant and controllable reflection coefficient to implement the desired tag modulation [14]. Without the loss of generality, to produce impedance values realizable with passive components, we assume that the effective signal  $[\mathbf{s}]_k \triangleq \frac{x_{\mathcal{T}_k} \sqrt{\alpha_k}}{|x_{\mathcal{T}_k}|}$  from  $\mathcal{T}_k$  satisfies  $\mathbb{E}\{[\mathbf{s}]_k^* [\mathbf{s}]_k\} = \alpha_k \in [0, 1], \forall k \in \mathcal{M}$ , because the scaling factor can be included in the  $\mathcal{T}_k$ 's reflection coefficient or BC  $\alpha_k$  definition [15]. Here, higher values of  $\alpha_k, \forall k \in \mathcal{M}$ , imply reflecting larger fraction of the incident RF power back to  $\mathcal{R}$ , which thus, results in higher backscattered signal strength, and thereby, maximizing the overall read-range of  $\mathcal{R}$ . Whereas, the lower value of BC for a tag implies that its backscattering to  $\mathcal{R}$  causes lesser interference for the other tags. Therefore, the baseband received signal  $[\mathbf{y}_{\mathcal{T}}]_k \in \mathbb{C}$  at  $\mathcal{T}_k$  can be expressed as:

$$[\mathbf{y}_{\mathcal{T}}]_k = \mathbf{h}_k^T \sum_{m \in \mathcal{M}} \mathbf{f}_m [\mathbf{s}_{\mathcal{R}}]_m + [\mathbf{w}_{\mathcal{T}}]_k, \quad \forall k \in \mathcal{M}, \quad (1)$$

where  $\mathbf{w}_{\mathcal{T}} \in \mathbb{C}^{N \times 1}$  represents zero-mean Additive White Gaussian Noise (AWGN) vector with IID entries, each having variance  $\sigma_{\mathbf{w}_{\mathcal{T}}}^2$ .

## 3. SUM THROUGHOUT MAXIMIZATION IN BSC

Here after presenting the backscattered-throughput expression and SBT maximization problem, we outline two TRX design properties.

### 3.1. Backscattered Throughput at Multiantenna Reader

Noting that the backscattered noise strength due to the AWGN power is practically negligible in comparison to the corresponding carrier reflection strength due the signal power, the received signal  $\mathbf{y}_{\mathcal{R}}$  at  $\mathcal{R}$  for information decoding, as obtained using (1), can be written as:

$$\mathbf{y}_{\mathcal{R}} \triangleq \sum_{m \in \mathcal{M}} \mathbf{h}_m [\mathbf{s}]_m [\mathbf{y}_{\mathcal{T}}]_m + \mathbf{w}_{\mathcal{R}}, \quad (2)$$

where  $\mathbf{w}_{\mathcal{R}} \sim \mathcal{CN}(\mathbf{0}_{N \times 1}, \sigma_{\mathbf{w}_{\mathcal{R}}}^2 \mathbf{I}_N)$  represents AWGN at  $\mathcal{R}$ . After applying the linear detection to  $\mathbf{y}_{\mathcal{R}}$ , the resulting decoded signal is:

$$\hat{\mathbf{y}}_{\mathcal{R}} \triangleq \mathbf{G}^H \mathbf{y}_{\mathcal{R}} = [\mathbf{g}_1 \ \mathbf{g}_2 \ \dots \ \mathbf{g}_M]^H \mathbf{y}_{\mathcal{R}}. \quad (3)$$

Therefore, on using (3), the resulting signal-to-interference-plus-noise-ratio (SINR)  $\gamma_{\mathcal{R}_k}$  for the backscattered message  $[\mathbf{s}]_k, \forall k \in \mathcal{M}$ , as received at  $\mathcal{R}$  from each  $\mathcal{T}_k$  can be derived as follows:

$$\gamma_{\mathcal{R}_k} \triangleq \frac{\alpha_k |\mathbf{g}_k^H \mathbf{h}_k|^2 \sum_{m \in \mathcal{M}} |\mathbf{h}_k^T \mathbf{f}_m|^2}{\sum_{i \in \mathcal{M}_k} \alpha_i |\mathbf{g}_k^H \mathbf{h}_i|^2 \sum_{m \in \mathcal{M}} |\mathbf{h}_i^T \mathbf{f}_m|^2 + \sigma_{\mathbf{w}_{\mathcal{R}}}^2 \|\mathbf{g}_k\|^2}, \quad (4)$$

where  $\mathcal{M}_k \triangleq \mathcal{M} \setminus \{k\}$ . Thus, on using (4), the backscattered-throughput  $R_k$  for tag  $\mathcal{T}_k$  as achieved at  $\mathcal{R}$  can be obtained as below:

$$R_k = \log_2(1 + \gamma_{\mathcal{R}_k}), \quad \forall k \in \mathcal{M}. \quad (5)$$

We aim to maximize the sum of  $R_k$ s to optimize the utility of  $\mathcal{R}$ .

### 3.2. Mathematical Formulation for SBT Maximization

The joint reader's TRX and tags' BC design problem is defined by:

$$\begin{aligned} \mathcal{O}_S : \quad & \max_{(\mathbf{f}_k, \mathbf{g}_k, \alpha_k), \forall k \in \mathcal{M}} R_S \triangleq \sum_{k \in \mathcal{M}} R_k, \quad \text{subject to (s.t.)} \\ \text{(C1)} : \quad & \sum_{k \in \mathcal{M}} \|\mathbf{f}_k\|^2 \leq P_T, \quad \text{(C2)} : \|\mathbf{g}_k\|^2 \leq 1, \forall k \in \mathcal{M}, \\ \text{(C3)} : \quad & \alpha_k \geq \alpha_{\min}, \forall k \in \mathcal{M}, \quad \text{(C4)} : \alpha_k \leq \alpha_{\max}, \forall k \in \mathcal{M}, \end{aligned}$$

where  $P_T$  is the available transmit power budget at  $\mathcal{R}$ ,  $\alpha_{\min} \geq 0$  and  $\alpha_{\max} \leq 1$  respectively the practically-realizable [15, 16] lower and upper bounds on BC  $\alpha \triangleq [\alpha_1 \ \alpha_2 \ \alpha_3 \ \dots \ \alpha_M]^T \in \mathbb{R}_{\geq 0}^{M \times 1}$ . Although  $\mathcal{O}_S$  has convex constraints, in general, it is a nonconvex problem because its nonconcave objective includes coupled terms involving the product of optimization variables, i.e., precoders  $\mathbf{f}_k$ , detectors  $\mathbf{g}_k$ , and BC  $\alpha_k, \forall k \in \mathcal{M}$ . Despite the non-convexity of joint optimization problem  $\mathcal{O}_S$ , we next reveal two key features of the underlying optimal TRX design, which will be used in Section 4.

**Lemma 1.** *The optimal TX precoders for  $M$  tags, that maximize the resulting SBT  $R_S$ , are identical, i.e.,  $\mathbf{f}_k = \frac{1}{\sqrt{M}} \mathbf{f} \in \mathbb{C}^{N \times 1}, \forall k \in \mathcal{M}$ .*

*Proof.* For a given detector  $\mathbf{g}_k$  and BC design  $\alpha_k, \forall k \in \mathcal{M}$ , the optimal precoders can be obtained by solving subgradient Karush Kuhn Tucker (KKT) condition [17, Ch. 5.5.3]  $\frac{\partial \mathcal{L}}{\partial \mathbf{f}_k} = \frac{\partial R_S}{\partial \mathbf{f}_k} - \nu \mathbf{f}_k = \mathbf{0}_{N \times 1}$  in terms of  $\mathbf{f}_k, \forall k \in \mathcal{M}$ , where  $\mathcal{L} = R_S + \nu (P_T - \sum_{k \in \mathcal{M}} \|\mathbf{f}_k\|^2)$  is Lagrangian function of  $\mathcal{O}_S$ , with  $\nu \geq 0$  being Lagrange multiplier for (C1). We can rewrite this condition as:  $\mathbf{f}_k = \sum_{m \in \mathcal{M}} \mathbf{Z}_m \mathbf{f}_k$ , with

$$\mathbf{Z}_m \triangleq \frac{\alpha_m |\mathbf{g}_m^H \mathbf{h}_m|^2 \mathbf{h}_m^* \mathbf{h}_m^T - \gamma_{\mathcal{R}_m} \sum_{i \in \mathcal{M}_m} \alpha_i |\mathbf{g}_m^H \mathbf{h}_i|^2 \mathbf{h}_i^* \mathbf{h}_i^T}{\nu \ln(2) \left( \sum_{i \in \mathcal{M}} \alpha_i |\mathbf{g}_m^H \mathbf{h}_i|^2 \left| \mathbf{h}_i^T \sum_{m \in \mathcal{M}} \mathbf{f}_m \right|^2 + \sigma_{\mathbf{w}_{\mathcal{R}}}^2 \|\mathbf{g}_m\|^2 \right)}. \quad (6)$$

Hence, this proves that the optimal precoder, denoted by  $\mathbf{f} \in \mathbb{C}^{N \times 1}$ , is identical for all tags, and we can write  $\mathbf{f}_k = \frac{1}{\sqrt{M}} \mathbf{f}, \forall k \in \mathcal{M}$ .  $\square$

Lemma 1 implies that  $\mathcal{R}$  transmits with same precoder  $\mathbf{f}$  for all the tags, i.e., *multicasting is optimal TX design*. A similar observation has also been made in context of precoder design in WPCN [9].

**Lemma 2.** *For a given precoder design  $\mathbf{f}_k = \frac{\mathbf{f}}{\sqrt{M}}, \forall k \in \mathcal{M}$ , for  $\mathcal{R}$  and BC vector  $\alpha$  for the tags, the optimal detector design  $\mathbf{g}_{\text{opt}k}, \forall k \in \mathcal{M}$  is characterized by the Wiener or MMSE filter, as defined below:*

$$\mathbf{g}_{\text{opt}k} = \frac{\left( \mathbf{I}_N + \frac{1}{\sigma_{\mathbf{w}_{\mathcal{R}}}^2} \sum_{i=1}^M \alpha_i |\mathbf{h}_i^T \mathbf{f}|^2 \mathbf{h}_i \mathbf{h}_i^H \right)^{-1} \mathbf{h}_k}{\left\| \left( \mathbf{I}_N + \frac{1}{\sigma_{\mathbf{w}_{\mathcal{R}}}^2} \sum_{i=1}^M \alpha_i |\mathbf{h}_i^T \mathbf{f}|^2 \mathbf{h}_i \mathbf{h}_i^H \right)^{-1} \mathbf{h}_k \right\|}. \quad (7)$$

*Proof.* Firstly, from (4) and (5) we notice that  $R_k$  for each  $\mathcal{T}_k$  depends only on its own detector  $\mathbf{g}_k$ . So, we can maximize the individual rates  $R_k$  or SINRs  $\gamma_{\mathcal{R}_k}$  in parallel with respect to  $\mathbf{g}_k$ , while satisfying their underlying normalization constraint (C2). Further, as the  $\gamma_{\mathcal{R}_k}$  in (4) can be alternately represented as a generalized Rayleigh

quotient form [18, eq. (16)], the optimal detector  $\mathbf{g}_{\text{op}_k}, \forall k \in \mathcal{M}$ , can be obtained as the generalized eigenvector of the matrix set  $\left( \frac{\alpha_k |\mathbf{h}_k^T \mathbf{f}|^2 \mathbf{h}_k \mathbf{h}_k^H}{\sigma_{\text{w}\mathcal{R}}^2}, \sum_{i \in \mathcal{M}_k} \frac{\alpha_i |\mathbf{h}_i^T \mathbf{f}|^2 \mathbf{h}_i \mathbf{h}_i^H}{\sigma_{\text{w}\mathcal{R}}^2} + \mathbf{I}_N \right)$  with largest eigenvalue. Using it along with (C2), the optimal detector in (7) is obtained.  $\square$

#### 4. NOVEL ASYMPTOTICALLY-OPTIMAL JOINT DESIGNS

Our proposed joint TRX-BC design is obtained by first deriving the asymptotically-optimal joint solutions in the high and low SNR regimes and then selecting the one which yields higher SBT. Next we discourse how they can be obtained with very low-complexity by exploiting the semi-closed-form expressions for RX and BC designs.

##### 4.1. TRX and BC Optimization Under High-SNR Regime

First from Lemma 2 we revisit that regardless of the precoder and BC design, the optimal detector is characterized by the MMSE filtering defined in (7). Next, we recall that under the high-SNR regime, the ZF-based RX beamforming is known to be a very good approximation for the Wiener or MMSE filter [18, eq. (14)]. So, defining the combined channel matrix as  $\mathbf{H} \triangleq [\mathbf{h}_1 \ \mathbf{h}_2 \ \mathbf{h}_3 \ \dots \ \mathbf{h}_M]$ , the optimal detector for the high-SNR scenarios is defined below:

$$\mathbf{g}_{\text{H}_k} \triangleq \frac{|\mathbf{G}_Z|_k}{\|\mathbf{G}_Z\|}, \forall k \in \mathcal{M}, \text{ with } \mathbf{G}_Z = \mathbf{H} (\mathbf{H}^H \mathbf{H})^{-1}. \quad (8)$$

Thus, with  $\tilde{\gamma}_{\text{g}_k} \triangleq \sigma_{\text{w}\mathcal{R}}^{-2} \|\mathbf{G}_Z\|_k^{-2}, \forall k \in \mathcal{M}$ , SBT under high-SNR regime for ZF based detector,  $\mathbf{G}_\text{H} \triangleq [\mathbf{g}_{\text{H}_1} \ \mathbf{g}_{\text{H}_2} \ \dots \ \mathbf{g}_{\text{H}_M}]$ , is:

$$\text{R}_{\text{S}_\text{H}} \triangleq \sum_{k \in \mathcal{M}} \log_2 \left( 1 + \alpha_k \tilde{\gamma}_{\text{g}_k} |\mathbf{h}_k^T \mathbf{f}|^2 \right), \quad (9)$$

where we have used Lemma 1 to set same TX precoder for all tags. Next using  $\mathcal{F} \triangleq \mathbf{f} \mathbf{f}^H$ , the equivalent semidefinite relaxation (SDR) is formulated as  $\mathcal{O}_\text{H}$ , and then Lemma 3 outlines a key result for it.

$$\mathcal{O}_\text{H}: \max_{\mathcal{F}, \alpha} \bar{\text{R}}_{\text{S}_\text{H}} \triangleq \sum_{k \in \mathcal{M}} \log_2 (1 + \alpha_k \tilde{\gamma}_{\text{g}_k} \mathbf{h}_k^T \mathcal{F} \mathbf{h}_k^*), \text{ s. t. (C3), (C4),}$$

$$(C5): \text{Tr}(\mathcal{F}) \leq P_T, (C6): \mathcal{F} \succeq 0, (C7): \text{rank}(\mathcal{F}) = 1.$$

**Lemma 3.**  $\bar{\text{R}}_{\text{S}_\text{H}}$  is concave in  $\mathcal{F}$  with optimal  $\alpha_k = \alpha_{\text{max}}, \forall k \in \mathcal{M}$ .

*Proof.* Firstly, we note that regardless of the value of  $\mathcal{F}$ ,  $\bar{\text{R}}_{\text{S}_\text{H}}$  is monotonically increasing in each  $\alpha_k, \forall k \in \mathcal{M}$ . So, optimal BC under high-SNR scenario is given by  $\alpha_{\text{H}_k} = \alpha_{\text{max}}, \forall k \in \mathcal{M}$ . Now, with both  $\alpha = \alpha_{\text{H}} \triangleq \alpha_{\text{max}} \mathbf{1}_{M \times 1}$  and  $\mathbf{G} = \mathbf{G}_\text{H}$  obtained, we next show that  $\mathcal{O}_\text{H}$  involves the maximization of sum of  $M$  concave functions  $\bar{\text{R}}_{\text{H}_k} \triangleq \log_2 (1 + \alpha_k \tilde{\gamma}_{\text{g}_k} \mathbf{h}_k^T \mathcal{F} \mathbf{h}_k^*), \forall k \in \mathcal{M}$  over the variable  $\mathcal{F}$ . Here, the concavity of each throughput term  $\bar{\text{R}}_{\text{H}_k}$  can be observed from the fact that it is a concave monotonically increasing (logarithmic) transformation of an affine function of  $\mathcal{F}$ .  $\square$

Using Lemma 3 and ignoring (C7), we notice that  $\mathcal{O}_\text{H}$  with  $\alpha_k = \alpha_{\text{max}}, \forall k \in \mathcal{M}$ , is a convex problem in the variable  $\mathcal{F}$ . Further, since this problem satisfies the DCP rule [19], the CVX toolbox can be used to obtain the optimal  $\mathcal{F}$ , as denoted by  $\mathcal{F}_\text{H}$ . However, for this precoding solution to satisfy the rank-one constraint (C7) we need to deploy the randomization process, which first involves the generation of  $K$  set of candidate weight vectors for  $\mathbf{f}$  using each of the three methods, namely randA, randB, and randC, as described in [20, Sec. IV]. Thereafter, the optimal precoder, denoted by  $\mathbf{f}_\text{H}$ , is selected as the one yielding highest  $\text{R}_{\text{S}_\text{H}}$  among the  $3K$  candidates.

**Remark 1.** Under high-SNR regime, optimal precoder  $\mathbf{f}_\text{H}$  is obtained by solving SDR  $\mathcal{O}_\text{H}$ , with all the tags being in full reflection mode  $\alpha_{\text{H}_k} = \alpha_{\text{max}}, \forall k \in \mathcal{M}$ , followed by randomization process. Whereas, the optimal detector follows ZF based design  $\mathbf{G} = \mathbf{G}_\text{H}$ .

##### 4.2. Proposed TRX-BC Design For Low-SNR Applications

Under low-SNR regime, the following two conditions hold good:

$$\sum_{i \in \mathcal{M}_k} \alpha_i |\mathbf{g}_k^H \mathbf{h}_i|^2 |\mathbf{h}_i^T \mathbf{f}|^2 + \sigma_{\text{w}\mathcal{R}}^2 \|\mathbf{g}_k\|^2 \approx \sigma_{\text{w}\mathcal{R}}^2 \|\mathbf{g}_k\|^2, \forall k \in \mathcal{M}, \quad (10a)$$

$$\sum_{k \in \mathcal{M}} \log_2 \left( 1 + \frac{\alpha_k |\mathbf{g}_k^H \mathbf{h}_k|^2 |\mathbf{h}_k^T \mathbf{f}|^2}{\sigma_{\text{w}\mathcal{R}}^2 \|\mathbf{g}_k\|^2} \right) \approx \sum_{k \in \mathcal{M}} \frac{\alpha_k |\mathbf{g}_k^H \mathbf{h}_k|^2 |\mathbf{h}_k^T \mathbf{f}|^2}{\sigma_{\text{w}\mathcal{R}}^2 \|\mathbf{g}_k\|^2 \ln(2)}. \quad (10b)$$

where (10a) is owing to the fact that under low-SNR regime, the backscattered signals from all the other tags, causing interference to the tag of interest, is relatively very low in comparison to the received AWGN. Whereas, (10b) is obtained using the identity  $\log_2(1+x) \approx \frac{x}{\ln(2)}, \forall x \ll 1$ . Using these two properties, the SBT to be maximized in precoder  $\mathbf{f}$  under low-SNR regime reduces to:

$$\text{R}_{\text{S}_\text{L}} = \sum_{k \in \mathcal{M}} \frac{\alpha_k |\mathbf{g}_k^H \mathbf{h}_k|^2 |\mathbf{h}_k^T \mathbf{f}|^2}{\ln(2) \sigma_{\text{w}\mathcal{R}}^2 \|\mathbf{g}_k\|^2} \stackrel{(r1)}{\leq} \frac{\alpha_{\text{max}} \text{Tr}\{\mathbf{H}^T \mathbf{f} \mathbf{f}^H \mathbf{H}^*\}}{\ln(2) \sigma_{\text{w}\mathcal{R}}^2}. \quad (11)$$

where (r1) is based on the individual optimizations of detector and BC vector, respectively, following MRC and full-reflection mode for low-SNR case. From (11), we notice that the TX precoder design  $\mathbf{f}$  maximizing sum received power also eventually yields the maximum SBT. Thus, the optimal precoder, called TX-EB, is given by:

$$\mathbf{f}_\text{L} \triangleq \sqrt{P_T} \frac{\mathbf{v}_{\text{max}}\{\mathbf{H}^* \mathbf{H}^T\}}{\|\mathbf{v}_{\text{max}}\{\mathbf{H}^* \mathbf{H}^T\}\|}, \quad (12)$$

where  $\mathbf{v}_{\text{max}}\{\mathbf{H}^* \mathbf{H}^T\}$  is the right singular vector of the matrix  $\mathbf{H}^* \mathbf{H}^T$  that corresponds to its maximum eigenvalue  $\lambda_{\text{max}}\{\mathbf{H}^* \mathbf{H}^T\}$ . On substituting  $\mathbf{f} = \mathbf{f}_\text{L}$  and  $\alpha_k = \alpha_{\text{max}}, \forall k \in \mathcal{M}$ , in (7) and using Lemma 2, the optimal detector for the low-SNR regime is given by:

$$\mathbf{g}_{\text{L}_k} \triangleq \frac{\left( \mathbf{I}_N + \frac{P_T \alpha_{\text{max}}}{\sigma_{\text{w}\mathcal{R}}^2} \sum_{i=1}^M |\mathbf{h}_i^T \mathbf{v}_{\text{max}}\{\mathbf{H}^* \mathbf{H}^T\}|^2 \mathbf{h}_i \mathbf{h}_i^H \right)^{-1} \mathbf{h}_k}{\left\| \left( \mathbf{I}_N + \frac{P_T \alpha_{\text{max}}}{\sigma_{\text{w}\mathcal{R}}^2} \sum_{i=1}^M |\mathbf{h}_i^T \mathbf{v}_{\text{max}}\{\mathbf{H}^* \mathbf{H}^T\}|^2 \mathbf{h}_i \mathbf{h}_i^H \right)^{-1} \mathbf{h}_k \right\|}. \quad (13)$$

With TRX designs obtained, BC optimization can be formulated as:

$$\mathcal{O}_{\text{BL}}: \max_{\alpha} \frac{1}{\ln(2)} \sum_{k \in \mathcal{M}} \frac{\alpha_k |\mathbf{g}_{\text{L}_k}^H \mathbf{h}_k|^2 |\mathbf{h}_k^T \mathbf{f}_\text{L}|^2}{\sum_{i \in \mathcal{M}_k} \alpha_i |\mathbf{g}_{\text{L}_k}^H \mathbf{h}_i|^2 |\mathbf{h}_i^T \mathbf{f}_\text{L}|^2 + \sigma_{\text{w}\mathcal{R}}^2}, \text{ s. t. (C3), (C4),}$$

with its asymptotically-optimal solution  $\alpha_\text{L}$  given by Lemma 4.

**Lemma 4.** For low-SNR settings, the optimal BC for each  $\mathcal{T}_k$  is only characterized either by  $\alpha_{\text{max}}$  or  $\alpha_{\text{min}}$ , i.e., follows ON-OFF mode.

*Proof.* First using the result below in (14), we show that  $\gamma_{\mathcal{R}_k}^{\text{sum}} \triangleq \sum_{k \in \mathcal{M}} \gamma_{\mathcal{R}_k}$  is strictly-convex function of BC  $\alpha_k$  of each tag  $\mathcal{T}_k$ ,

$$\frac{\partial^2 \gamma_{\mathcal{R}_k}^{\text{sum}}}{\partial \alpha_k^2} = \sum_{i \in \mathcal{M}_k} \frac{2 \left( |\mathbf{h}_k^T \mathbf{f}|^2 \sigma_{\text{w}\mathcal{R}}^{-2} |\mathbf{g}_{\text{L}_k}^H \mathbf{h}_k|^2 \right)^2 \alpha_i |\mathbf{h}_i^T \mathbf{f}_\text{L}|^2 |\mathbf{g}_{\text{L}_i}^H \mathbf{h}_i|^2}{\left( \sum_{m \in \mathcal{M}_i} \alpha_m |\mathbf{h}_m^T \mathbf{f}_\text{L}|^2 |\mathbf{g}_{\text{L}_i}^H \mathbf{h}_m|^2 + \sigma_{\text{w}\mathcal{R}}^2 \right)^3} > 0. \quad (14)$$

Next since we aim to maximize the scaled  $\gamma_{\mathcal{R}_k}^{\text{sum}}$  in  $\mathcal{O}_{\text{BL}}$  and the maximum value of a convex function lies at the corner of its underlying variable, we conclude that the optimal value of each  $\alpha_k$  is set to either one out of the two corner points,  $\alpha_{\text{max}}$  or  $\alpha_{\text{min}}$ , for BC.  $\square$

Below we summarize, the joint TRX-BC design in low SNR regime.

**Remark 2.** Under low-SNR regime, precoding  $\mathbf{f}_\text{L}$  reduces to TX-EB and detector design follows MMSE filtering (cf. (13)). Whereas, BC optimization reduces to a low-complexity binary decision-making process, in which just  $2^M - 1$  possible candidates need to be checked for  $\alpha$  to select the best  $\alpha_\text{L}$  among them in terms of sum throughput.

Hence, via Remarks 1 and 2, we have described our two candidates for the joint solution, with RX and BC designs being in closed-form. So, only TX precoder is numerically computed using SDR and eigenvalue-decomposition respectively for high and low-SNR cases.

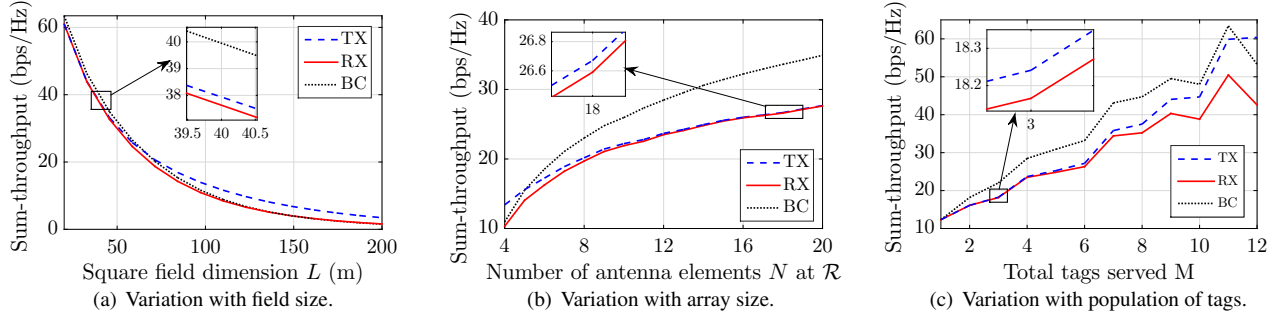


**Fig. 1.** Investigating the relative performance of the proposed optimal TX precoder, RX detector, and BC designs.

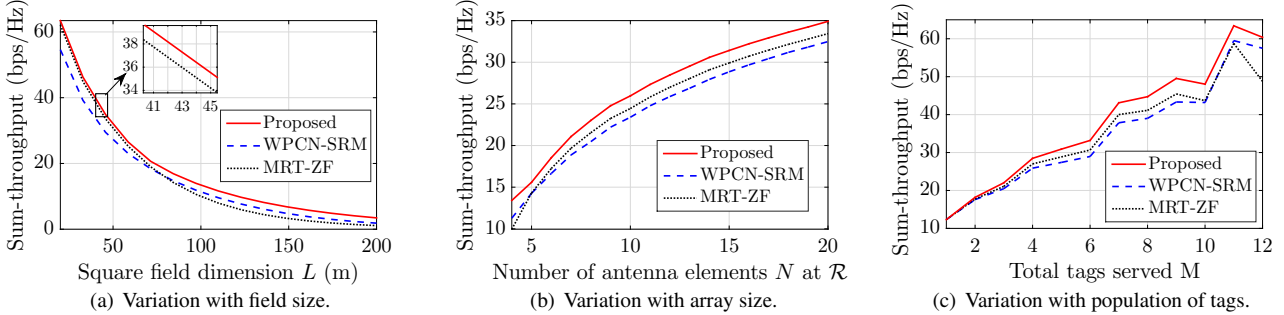


**Fig. 2.** Sum-throughput performance comparison of the proposed low-complexity joint TRX design against the relevant benchmarks.

## 5. NUMERICAL PERFORMANCE EVALUATION

Unless explicitly stated, we have used  $N = M = 4$ ,  $P_T = 1\text{W}$ ,  $\sigma_{w_T}^2 = \sigma_{w_R}^2 = 10^{-17}\text{W}$ ,  $K = 10NM$ , and  $\beta_i = \varpi d_i^{-\varrho}$ ,  $\forall i$ , where  $\varpi = \left(\frac{3 \times 10^8}{4\pi f}\right)^2$  being the average channel attenuation at unit reference distance with  $f = 915\text{MHz}$  [16] being TX frequency,  $d_i$  is  $\mathcal{R}$ -to- $\mathcal{T}_i$  distance, and  $\varrho = 3$  is path loss exponent. Noting the practical settings for BC designing [15] as  $\max\{|x_{\mathcal{T}_k}|\} = 0.78$  [2] and  $\mathbb{E}\{|x_{\mathcal{T}_k}|\} = 0.3162$  [13], we set  $\alpha_{\min} = 0.1 (\mathbb{E}\{|x_{\mathcal{T}_k}|\})^2 = 0.01$  and  $\alpha_{\max} = \max\{|x_{\mathcal{T}_k}|\} (\mathbb{E}\{|x_{\mathcal{T}_k}|\})^2 = 0.078$ ,  $\forall k \in \mathcal{M}$ . Regarding deployment,  $M$  tags have been placed uniformly over a square field of length  $L = 100\text{m}$  and  $\mathcal{R}$  is placed at its center. Lastly, all the optimal SBT results have been obtained numerically after taking average over  $10^3$  independent channel fading realizations.

First we conduct a relative performance comparison study among the three semi-adaptive designs involving individual optimizations of TX precoding, RX beamforming, and BC vector, for different values of  $L$ ,  $N$ , and  $M$  in Figs. 1(a), 1(b), and 1(c), respectively. For individual optimizations here we have used fixed TX precoding as  $\mathbf{f}_L$  (EB design), detector as  $\mathbf{G}_H$  (ZF-based RX beamforming design), and BC vector as  $\alpha_H$  (full reflection mode). From Fig. 1(a), we notice that the optimal TX precoding with fixed  $\mathbf{G} = \mathbf{G}_H$  and  $\alpha = \alpha_H$  performs better than the other two semi-adaptive designs for higher values of  $L$  with  $N = M = 4$ . Whereas, with optimal RX beamforming design being the weakest scheme as observed in Fig. 1, it implies that MMSE-based design is not that critical and in fact ZF-based asymptotically-optimal one is practically good enough. Furthermore, the optimal BC design having TX-EB as precoder and ZF-based RX-beamforming turns out to be the best semi-adaptive scheme, except under very low SNR regimes, as represented via  $L \geq 70\text{m}$ ,  $N \leq 5$ , and  $M \geq 12$  in Fig. 1.

Finally, to corroborate the practical utility of the proposed designs, we compare their performance against the two available benchmark designs, namely, (i) WPCN-SRM scheme [10] targeted towards the TRX designing at the multiantenna HAP for the uplink sum-rate-maximization (SRM) from the multiple single-antenna EH

users, and (ii) MRT-ZF scheme [5, 7] where the maximum ratio transmission (MRT) based precoder and ZF based detector are designed for each tag. As both these benchmarks do not consider BC optimization and use  $\alpha = \alpha_H$ , for fair comparison we consider the proposed asymptotically-optimal TRX design with fixed BC as  $\alpha_H$ . The performance comparison results for the two proposals against the two benchmarks are plotted in Figs. 2(a), 2(b), and 2(c) for varying  $L$ ,  $N$ , and  $M$ , respectively. It is clearly visible that even the proposed asymptotically-optimal TRX design with fixed BC  $\alpha_H$  outperforms both the benchmarks, respectively provides an average improvement of about 18% and 28% over the MRT-ZF and WPCN-SRM schemes in terms of achievable SBT. The main reasons for this significant improvement are that the TX-EB based common precoding design performs much better in terms of SBT than the respective suboptimal MRT design for each tag as proposed in [5, 7], and that the TX precoder of WPCN-SRM scheme with MMSE-RX which is aimed at optimizing a nonequivalent goal as defined in [10, Prop. 1]. Further, to quantify the performance gap between the proposed and optimal solutions, the extended version of this work investigates a joint TRX-BC design that holds good for all the SNR values [21].

## 6. CONCLUDING REMARKS

This work investigated novel sum-backscattered-throughput maximization problem that jointly optimizes the TRX design at the multi-antenna  $\mathcal{R}$  and BC at the single antenna tags. We showed that the optimal TX precoding is based on the direction that trade-offs between the one maximizing sum-received power among the tags and the one balancing among individual MRT direction for each tag. Whereas the detector design is based on MMSE beamforming and the BC optimization reduces to a low-complexity binary decision-making process. Numerical investigation validating the near-optimality of the asymptotically-optimal low-complexity designs for both low and high SNR regimes, showed that the proposed solutions can yield an overall enhancement of around 20% over benchmark schemes. In future, we would like to extend these low-complexity TRX and BC designs for fairness maximization among multiantenna tags in BSC.

## 7. REFERENCES

- [1] C. Xu, L. Yang, and P. Zhang, "Practical backscatter communication systems for battery-free Internet of Things: A tutorial and survey of recent research," *IEEE Signal Process. Mag.*, vol. 35, no. 5, pp. 16–27, Sept. 2018.
- [2] A. Bekkali, S. Zou, A. Kadri, M. Crisp, and R. V. Penty, "Performance analysis of passive UHF RFID systems under cascaded fading channels and interference effects," *IEEE Trans. Wireless Commun.*, vol. 14, no. 3, pp. 1421–1433, Mar. 2015.
- [3] C. Boyer and S. Roy, "Invited paper – Backscatter communication and RFID: Coding, Energy, and MIMO analysis," *IEEE Trans. Commun.*, vol. 62, no. 3, pp. 770–785, Mar. 2014.
- [4] G. Zhu, S. Ko, and K. Huang, "Inference from randomized transmissions by many backscatter sensors," *IEEE Trans. Wireless Commun.*, vol. 17, no. 5, pp. 3111–3127, May 2018.
- [5] G. Yang, Q. Zhang, and Y. C. Liang, "Cooperative ambient backscatter communications for green internet-of-things," *IEEE Internet Things J.*, vol. 5, no. 2, pp. 1116–1130, Apr. 2018.
- [6] D. Mishra and E. G. Larsson, "Optimal channel estimation for reciprocity-based backscattering with a full-duplex MIMO reader," *IEEE Trans. Signal Process.*, vol. 67, no. 6, pp. 1662–1677, Mar. 2019.
- [7] G. Yang, C. K. Ho, and Y. L. Guan, "Multi-antenna wireless energy transfer for backscatter communication systems," *IEEE J. Sel. Areas Commun.*, vol. 33, no. 12, pp. 2974–2987, Dec. 2015.
- [8] G. Yang, C. K. Ho, R. Zhang, and Y. L. Guan, "Throughput optimization for massive MIMO systems powered by wireless energy transfer," *IEEE J. Sel. Areas Commun.*, vol. 33, no. 8, pp. 1640–1650, Aug. 2015.
- [9] H. Lee, K. Lee, H. Kong, and I. Lee, "Sum-rate maximization for multiuser MIMO wireless powered communication networks," *IEEE Trans. Veh. Technol.*, vol. 65, no. 11, pp. 9420–9424, Nov. 2016.
- [10] D. Hwang, D. I. Kim, and T. Lee, "Throughput maximization for multiuser MIMO wireless powered communication networks," *IEEE Trans. Veh. Technol.*, vol. 65, no. 7, pp. 5743–5748, July 2016.
- [11] I. Krikidis, "Retrodirective large antenna energy beamforming in backscatter multi-user networks," *IEEE Wireless Commun. Lett.*, vol. 7, no. 4, pp. 678–681, Aug. 2018.
- [12] D. P. Villame and J. S. Marciano, "Carrier suppression locked loop mechanism for UHF RFID readers," in *Proc. IEEE Int. Conf. RFID*, Orlando, FL, USA, Apr. 2010, pp. 141–145.
- [13] J. Kimionis, A. Bletsas, and J. N. Sahalos, "Increased range bistatic scatter radio," *IEEE Trans. Commun.*, vol. 62, no. 3, pp. 1091–1104, Mar. 2014.
- [14] R. Correia, A. Boaventura, and N. B. Carvalho, "Quadrature amplitude backscatter modulator for passive wireless sensors in IoT applications," *IEEE Trans. Microw. Theory Techn.*, vol. 65, no. 4, pp. 1103–1110, Apr. 2017.
- [15] S. J. Thomas, E. Wheeler, J. Teizer, and M. S. Reynolds, "Quadrature amplitude modulated backscatter in passive and semipassive UHF RFID systems," *IEEE Trans. Microw. Theory Techn.*, vol. 60, no. 4, pp. 1175–1182, Apr. 2012.
- [16] D. Mishra and E. G. Larsson, "Optimizing reciprocity-based backscattering with a full-duplex antenna array reader," in *Proc. IEEE Int. Workshop Signal Process. Adv. Wireless Commun. (SPAWC)*, Kalamata, Greece, June 2018, pp. 1–5.
- [17] S. Boyd and L. Vandenberghe, *Convex Optimization*. Cambridge University Press, 2004.
- [18] E. Björnson, M. Bengtsson, and B. Ottersten, "Optimal multiuser transmit beamforming: A difficult problem with a simple solution structure [lecture notes]," *IEEE Signal Process. Mag.*, vol. 31, no. 4, pp. 142–148, July 2014.
- [19] M. Grant and S. Boyd, "CVX: Matlab software for disciplined convex programming," version 2.1. <http://cvxr.com/cvx>, Mar. 2014.
- [20] N. D. Sidiropoulos, T. N. Davidson, and Z.-Q. Luo, "Transmit beamforming for physical-layer multicasting," *IEEE Trans. Signal Process.*, vol. 54, no. 6, pp. 2239–2251, June 2006.
- [21] D. Mishra and E. G. Larsson, "Sum throughput maximization in multi-tag backscattering to multi-antenna reader," *IEEE Trans. Commun.*, Feb. 2019, under revision.